

# Active Fault-Tolerant Control System Design for Spacecraft Attitude Maneuvers with Actuator Saturation and Faults

Qiang Shen, *Member, IEEE*, Chengfei Yue, *Student Member, IEEE*, Cher Hiang Goh, *Senior Member, IEEE*, and Danwei Wang, *Senior Member, IEEE*

**Abstract**—This paper designs an active fault-tolerant control system for spacecraft attitude control in the presence of actuator faults, fault estimation errors, and control input constraints. The developed fault-tolerant control system is able to detect the actuator fault without false alarms caused by external disturbances, and also estimate the total fault effects accurately through an indirect fault identification approach, in which an auxiliary variable is utilized to build the relation between fault and system states. Once the fault identification is completed with certain degree of reconstruction accuracy, a fault-tolerant backstepping controller using the nonlinear virtual control input is re-configured to accommodate the detected actuator faults effectively, in spite of actuator saturation limitations and fault estimation errors. Numerical simulation is carried out to demonstrate that the proposed active fault-tolerant control system is successful in fault detection, identification, and controller reconfiguration for handling actuator faults in attitude control systems.

**Index Terms**—Actuators, Fault detection and identification, Fault-tolerant control, Saturation

## I. INTRODUCTION

FOR safety critical systems such as spacecraft and aircraft, it is important to possess a fault-tolerant control system (FTCS) to enhance reliability and ensure survivability as even a minor fault may lead to severe performance deterioration or mission failure. An FTCS is a control system that is capable of accommodating component faults automatically while maintaining overall closed-loop stability and control performance [1]–[3]. Recently, autonomous attitude control in the presence of actuator faults has received a great deal of attention in both aerospace engineering and academic communities due to the increasing demand for performance and capability of future spacecraft [4]. For spacecraft attitude control design in the

absence of actuator faults, several nonlinear control strategies, such as backstepping control [5]–[7], sliding mode control [8], [9], PD-type controller [10], [11], etc., have been proposed. To develop an FTCS for spacecraft attitude control system, two design approaches are generally available: passive FTCS and active FTCS [12].

In a passive FTCS for attitude control, a single fixed controller is synthesized to achieve the required attitude maneuvers not only in normal operating condition but also in fault mode. In [13], distributed controllers were proposed to solve attitude coordination control problem with consideration of actuator failures for spacecraft formation flying. In [14], integral sliding mode control strategy was employed to deal with partial loss of effectiveness fault and additive bias fault in spacecraft attitude stabilization. Based on fast terminal sliding mode control technique, finite-time convergence of the closed-loop trajectory and fault-tolerant capability were achieved in [15] for spacecraft attitude stabilization in spite of external disturbances, actuator saturation constraints, and actuator faults or failures. In [16], finite-time fuzzy sampled-data control for flexible spacecraft in the presence of stochastic actuator failures was studied, where a fuzzy switching FTC strategy was proposed to achieve  $H_\infty$  control performance and finite-time attitude stabilization. However, in comparison with the active FTCS approach, the passive one has limited fault-tolerant capacity as only specific pre-defined fault could be handled, although it is simple for implementation. In addition, most of passive FTCS strategies employ the upper bound of the fault to design the fault-tolerant controller, which is conservative from the control performance perspective and prone to reach the actuator saturation limit.

In contrast to the passive FTCS, the active FTCS consists of a fault detection and diagnosis (FDD) scheme providing fault information, a fault-tolerant controller compensating fault effects, and a decision mechanism deciding when and how to put reconfiguration controller into action. In [17], a sliding-mode observer was presented to estimate the angular velocity and actuator fault in the attitude control system, and a velocity-free attitude controller was further developed to stabilize the attitude asymptotically. In [18], a precise fault estimation is achieved via the nonlinear geometric approach with radial basis function neural networks. Then, the obtained fault information was used in an adaptive control allocation to handle actuator faults and maintain the desired control performance.

Manuscript received Month xx, 2xxx; revised Month xx, xxxx; accepted Month x, xxxx).

Qiang Shen is with the School for Engineering of Matter, Transport and Energy, Arizona State University, Tempe, AZ 85287, USA (e-mail: qiang.shen@hotmail.com).

Chengfei Yue and Cher Hiang Goh are with the Department of Electrical and Computer Engineering, National University of Singapore, Singapore 117583, Singapore (e-mail: chengfei\_yue@u.nus.edu; elegch@nus.edu.sg).

Danwei Wang is with the School of Electrical and Electronic Engineering, Nanyang Technological University, Singapore 639798, Singapore (e-mail: edwwang@ntu.edu.sg).

In [19], using an adaptive terminal sliding mode observer, the designed controller was able to handle actuator fault, systems uncertainties, and actuator saturation simultaneously despite the immeasurable states. In [20], local adaptive observers were designed to simultaneously identify two types of actuator faults for each individual actuator. Then, an adaptive fault-tolerant control approach consisting of a terminal sliding mode controller and a control allocation algorithm was proposed to achieve finite-time attitude stabilization.

In this paper, we focus on the active FTCS design for spacecraft attitude control with consideration of actuator faults, fault estimation errors, input saturation constraints, and external disturbances. To cope with potential actuator faults, a fault detection observer is firstly presented to detect the fault promptly, where the value of threshold for the detection residual is given explicitly. Then, an auxiliary parameter is introduced to establish the relation between angular velocity and total actuator faults. Based on the estimated values of angular velocity and auxiliary parameter from an indirect fault identification approach, the total fault effects influencing attitude control performance are obtained. Finally, despite control input saturation and fault estimation imperfection, a backstepping controller using a nonlinear virtual control signal is presented to accommodate actuator faults and maintain closed-loop stability. Comparing with the existing results, the main contributions are as follows:

- 1) We propose to estimate the total effect of the multiplicative and additive actuator fault instead of each fault individually. This makes the structure, computation, and design procedure relatively simple comparing with the existing result in [20], thus enhancing the availability in practical implementation, especially when computing power and onboard memory space are limited.
- 2) In view of the physical limitation of the actuator and the fault estimation imperfection caused by the limited time allocated to fault estimation in real spacecraft operation [15], we also consider actuator saturation constraint and the fault estimation error in fault-tolerant controller design.
- 3) Theoretically, a nonlinear virtual control input based on hyperbolic function is first developed in the fault-tolerant backstepping controller design. Comparing with the traditional backstepping controller [5], [6] using a linear virtual control input, it avoids the sluggish motion when the system state is near the equilibrium point.

The remainder of this paper is organized as follows. Section II briefly describes the spacecraft dynamics and introduces the fault model. Section III presents the proposed fault detection and estimation approaches. Section IV addresses the design procedure of the fault-tolerant controller. Subsequently, performance of the proposed FTCS is evaluated in Section V. Finally, concluding remarks are given in Sec. VI.

## II. PRELIMINARIES

The rigid spacecraft rotational equations are described mathematically by the kinematic and kinetic equations. In this paper, the unit-quaternion representation is used to describe

the orientation of a spacecraft as it represents all attitudes of a spacecraft globally and is well suited for onboard real-time computation [21].

### A. Spacecraft Attitude Dynamics

The equations of motion in terms of unit-quaternion for a rigid spacecraft are given by [22]

$$\mathbf{J}\dot{\boldsymbol{\omega}}_b = -\mathbf{S}(\boldsymbol{\omega}_b)\mathbf{J}\boldsymbol{\omega}_b + \mathbf{D}\mathbf{u} + \mathbf{d} \quad (1)$$

$$\dot{\mathbf{Q}} = \frac{1}{2} \begin{bmatrix} \mathbf{S}(\mathbf{q}) + q_0 \mathbf{I}_3 \\ -\mathbf{q}^T \end{bmatrix} \boldsymbol{\omega}_b, \quad (2)$$

where  $\mathbf{J} \in \mathbb{R}^{3 \times 3}$  denotes symmetric positive-definite inertia matrix, the vector  $\boldsymbol{\omega}_b \in \mathbb{R}^3$  is the angular velocity in the body-fixed frame,  $\mathbf{Q} = [q_1 \ q_2 \ q_3 \ q_0]^T = [\mathbf{q}^T \ q_0]^T \in \mathbb{R}^4$  denotes the unit-quaternion describing the orientation of the body-fixed frame  $\mathcal{B}$  with respect to inertial frame  $\mathcal{N}$ ,  $\mathbf{u} \in \mathbb{R}^n$  denotes the control torque produced by  $n$  actuators about the body axes,  $\mathbf{D} \in \mathbb{R}^{3 \times n}$  is the actuator configuration matrix,  $\mathbf{d} \in \mathbb{R}^3$  is the environmental disturbances. Noting that  $\mathbf{q}$  and  $q_0$  are the vector part and scalar part of the unit-quaternion satisfying  $\mathbf{q}^T \mathbf{q} + q_0^2 = 1$ , and the matrix  $\mathbf{S}(\mathbf{x}) \in \mathbb{R}^{3 \times 3}$  represents a skew-symmetric matrix for any vector  $\mathbf{x} \in \mathbb{R}^3$ .

### B. Actuator Fault Models

For spacecraft, reaction wheel and thruster are commonly used actuators in attitude control. For example, the reaction wheel is a flywheel attached with a motor, and fault may occur in electronics, drive motor, bearing, and power supply due to inadequate lubrication, aging, marginal failures, and increased friction. The following are four typical kinds of reaction wheel faults [14], [23]: (1) decreased reaction torque; (2) increased bias torque; (3) failure to respond to control signals; (4) continuous generation of reaction torque. These fault may affect the actuator output in a multiplicative or additive way. If one of these faults occurs, the reaction wheel may have a slower response, become less effective, and even undergo a complete breakdown.

Let  $\mathbf{u}_c \in \mathbb{R}^n$  be a vector denoting the command control torque. The relation between the command torque and the actual torque acting on the spacecraft is modelled as

$$\mathbf{u} = (\mathbf{I}_n - \mathbf{E})\mathbf{u}_c + \mathbf{u}_a, \quad (3)$$

where the matrix  $\mathbf{E} = \text{diag}\{e_1, e_2, \dots, e_n\} \in \mathbb{R}^{n \times n}$  describes the effectiveness loss of the actuators and its diagonal elements satisfies  $0 \leq e_i \leq 1, i \in \{1, 2, \dots, n\}$ . Noting that  $0 < e_i < 1$  indicates the  $i$ th actuator partially loses its effectiveness,  $e_i = 0$  implies the actuator is healthy, and  $e_i = 1$  implies the actuator totally failed. The variable  $\mathbf{u}_a = [u_{a1} \ u_{a2} \ \dots \ u_{an}]^T \in \mathbb{R}^n$  represents the additive bias fault. Substituting the fault model (3) into (1), the attitude dynamics considering actuator faults is written as follows:

$$\mathbf{J}\dot{\boldsymbol{\omega}}_b = -\mathbf{S}(\boldsymbol{\omega}_b)\mathbf{J}\boldsymbol{\omega}_b + \mathbf{D}\mathbf{u}_c + \mathbf{f} + \mathbf{d}, \quad (4)$$

where  $\mathbf{f} = -\mathbf{D}\mathbf{E}\mathbf{u}_c + \mathbf{D}\mathbf{u}_a$  denotes the total fault effects on the system.

The following Assumptions are used in the FTCS design.

**Assumption 1:** The inertia matrix  $\mathbf{J}$  satisfies the condition  $\underline{J} \leq \|\mathbf{J}\| \leq \bar{J}$ , where  $\underline{J}$  and  $\bar{J}$  are two positive constants. The symbol  $\|\cdot\|$  denotes the Euclidean norm and its induced norm.

**Assumption 2:** In practice, the environmental disturbances due to gravitation, solar radiation pressure, magnetic forces or aerodynamic drag are bounded. Therefore, there exists a positive constant  $\bar{d}$  such that  $\|\mathbf{d}\| \leq \bar{d}$ .

**Assumption 3:** It is assumed that the total fault effects representing by  $\mathbf{f}$  satisfy  $\|\mathbf{f}\| \leq \phi$ , where  $\phi$  is a constant.

**Remark 1:** As indicated in Assumption 3, we consider the slow-varying fault or incipient fault in this paper, which represents one of the typical faults existing in actuators. For example, faults causing by aging, temperature, lubrication or operational wear and tear may generate a gradually increased bias torque in reaction wheel [15]. It is also noted that the magnitude of additive fault  $\mathbf{u}_a$  cannot be arbitrarily large and is bounded at least by the physical limitation of actuators.

### C. Problem Statement

This paper aims to provide an active FTCS for spacecraft attitude maneuvers subject to external disturbances and actuator faults. Fig. 1 shows the structure of the overall proposed active FTCS. Regarding to the normal controller, there have been many results that can be applied to attitude control directly, for example controllers in [10], [24]. Therefore, we do not consider normal controller design in this paper, and only FDD and fault-tolerant controller are addressed. The FDD scheme contains fault detection and fault identification, which are utilized to obtain the actuator fault characterization including existence of the fault, the time at which fault occurs, and magnitude of the fault. The fault-tolerant controller is designed based on the fault information from the FDD scheme to accommodate actuator faults and maintain the control performance.

## III. FAULT DETECTION AND IDENTIFICATION

To get fault information with sufficient accuracy, both fault detection and fault identification approaches are developed in this section.

### A. Fault Detection

Based on the attitude dynamics in (1), the fault detection observer is designed as

$$\mathbf{J}\dot{\hat{\boldsymbol{\omega}}}_{b,d} = -\mathbf{S}(\hat{\boldsymbol{\omega}}_{b,d})\mathbf{J}\hat{\boldsymbol{\omega}}_{b,d} + \mathbf{D}\mathbf{u}_c + \mathbf{\Lambda}(\boldsymbol{\omega}_b - \hat{\boldsymbol{\omega}}_{b,d}), \quad (5)$$

where  $\hat{\boldsymbol{\omega}}_{b,d}$  is the estimate of the angular velocity  $\boldsymbol{\omega}_b$  in fault detection, and  $\mathbf{\Lambda} \in \mathbb{R}^{3 \times 3}$  is a positive gain matrix. Let  $\tilde{\boldsymbol{\omega}}_{b,d} = \boldsymbol{\omega}_b - \hat{\boldsymbol{\omega}}_{b,d}$  be the velocity estimation error, then it is obtained that

$$\mathbf{J}\dot{\tilde{\boldsymbol{\omega}}}_{b,d} = -\mathbf{S}(\boldsymbol{\omega}_b)\mathbf{J}\boldsymbol{\omega}_b + \mathbf{S}(\hat{\boldsymbol{\omega}}_{b,d})\mathbf{J}\hat{\boldsymbol{\omega}}_{b,d} - \mathbf{\Lambda}\tilde{\boldsymbol{\omega}}_{b,d} + \mathbf{f} + \mathbf{d}. \quad (6)$$

**Assumption 4:** The nonlinear term  $-\mathbf{S}(\boldsymbol{\omega}_b)\mathbf{J}\boldsymbol{\omega}_b + \mathbf{S}(\hat{\boldsymbol{\omega}}_{b,d})\mathbf{J}\hat{\boldsymbol{\omega}}_{b,d}$  in (6) is supposed to be known and satisfy the Lipschitz condition with respect to  $\tilde{\boldsymbol{\omega}}_{b,d}$ , i.e.,

$$\|-\mathbf{S}(\boldsymbol{\omega}_b)\mathbf{J}\boldsymbol{\omega}_b + \mathbf{S}(\hat{\boldsymbol{\omega}}_{b,d})\mathbf{J}\hat{\boldsymbol{\omega}}_{b,d}\| \leq \ell_g \|\tilde{\boldsymbol{\omega}}_{b,d}\|, \quad (7)$$

where  $\ell_g$  is the Lipschitz constant.

**Remark 2:** For practical functional spacecraft, the actual angular velocity is continuous and within a certain range to conduct some scientific missions. The attitude controller is designed to ensure attitude stabilization and angular velocity constraint, for example, attitude controllers in [25], [26]. Thus, the estimation of the bounded angular velocity should also be bounded. Therefore, the Lipschitz condition in Assumption 4 is reasonable, and the Lipschitz constant can be obtained in advance from the bounds of angular velocity and spacecraft inertia. Similar assumption of the Lipschitz condition in attitude control can also be found in [27].

Next, the estimation error  $\tilde{\boldsymbol{\omega}}_{b,d}$  is used to generate residual for fault detection. The decision method for actuator fault detection is stated in the following Theorem.

**Theorem 1:** The decision on the occurrence of actuator fault is made when the estimation error  $\tilde{\boldsymbol{\omega}}_b$  in (6) exceeds the threshold defined as  $\xi_{dt} = \frac{\bar{d}}{\lambda_{\min}[\mathbf{\Lambda}] - \ell_g}$ . That is, the actuator fault is detected if the condition  $\|\tilde{\boldsymbol{\omega}}_{b,d}\| > \xi_{dt}$  is satisfied.

*Proof.* Consider a Lyapunov candidate in the form of

$$V = \frac{1}{2} \tilde{\boldsymbol{\omega}}_{b,d}^T \mathbf{J} \tilde{\boldsymbol{\omega}}_{b,d}. \quad (8)$$

The time derivative of (8) along (6) is given as

$$\begin{aligned} \dot{V} &= \tilde{\boldsymbol{\omega}}_{b,d}^T (-\mathbf{S}(\boldsymbol{\omega}_b)\mathbf{J}\boldsymbol{\omega}_b + \mathbf{S}(\hat{\boldsymbol{\omega}}_{b,d})\mathbf{J}\hat{\boldsymbol{\omega}}_{b,d} - \mathbf{\Lambda}\tilde{\boldsymbol{\omega}}_{b,d} + \mathbf{f} + \mathbf{d}) \\ &\leq -(\lambda_{\min}[\mathbf{\Lambda}] - \ell_g) \|\tilde{\boldsymbol{\omega}}_{b,d}\|^2 + \bar{d} \|\tilde{\boldsymbol{\omega}}_{b,d}\| + \tilde{\boldsymbol{\omega}}_{b,d}^T \mathbf{f}. \end{aligned} \quad (9)$$

The notation  $\lambda_{\min}[\cdot]$  denotes the minimum eigenvalue of a matrix. If there is no actuator fault in the system, the fault does not affect the system, i.e., the total fault effect is  $\mathbf{f} = 0$ . In this case, the foregoing inequality becomes

$$\dot{V} \leq -(\lambda_{\min}[\mathbf{\Lambda}] - \ell_g) \|\tilde{\boldsymbol{\omega}}_{b,d}\|^2 + \bar{d} \|\tilde{\boldsymbol{\omega}}_{b,d}\| \quad (10)$$

It is clear that  $\dot{V} < 0$  if  $\|\tilde{\boldsymbol{\omega}}_{b,d}\| > \frac{\bar{d}}{\lambda_{\min}[\mathbf{\Lambda}] - \ell_g}$ . Supposing the initial condition of the fault detection observer is chosen to satisfy  $\hat{\boldsymbol{\omega}}_{b,d}(0) = \boldsymbol{\omega}_b(0)$ , it is obtained that  $\|\tilde{\boldsymbol{\omega}}_{b,d}\| \leq \frac{\bar{d}}{\lambda_{\min}[\mathbf{\Lambda}] - \ell_g}$  for all the time, which indicates that the error  $\tilde{\boldsymbol{\omega}}_{b,d}$  is upper bounded by a constant in the fault-free situation.

If a fault occurs, i.e.,  $\|\mathbf{f}\| \neq 0$ , it is observed that

$$\dot{V} \leq -(\lambda_{\min}[\mathbf{\Lambda}] - \ell_g) \|\tilde{\boldsymbol{\omega}}_{b,d}\|^2 + (\bar{d} + \|\mathbf{f}\|) \|\tilde{\boldsymbol{\omega}}_{b,d}\|. \quad (11)$$

Following the similar analysis in fault-free case, it yields

$$\|\tilde{\boldsymbol{\omega}}_{b,d}\| \leq \frac{\bar{d} + \|\mathbf{f}\|}{\lambda_{\min}[\mathbf{\Lambda}] - \ell_g}, \quad (12)$$

which implies that  $\|\tilde{\boldsymbol{\omega}}_{b,d}\|$  may exceed its maximal value in fault-free case. Therefore, a fault detection threshold can be set as  $\xi_{dt} = \frac{\bar{d}}{\lambda_{\min}[\mathbf{\Lambda}] - \ell_g}$ . The fault is detected if  $\|\tilde{\boldsymbol{\omega}}_{b,d}\| > \xi_{dt}$  is observed. This completes the proof.  $\triangle \triangle \triangle$

**Remark 3:** Theorem 1 provides a sufficient condition for fault detection. If the condition in Theorem 1 is satisfied, there must exist a fault in the system. However, the converse of this statement may not necessarily be true. Specifically, the inequality  $\|\tilde{\boldsymbol{\omega}}_{b,d}\| > \xi_{dt}$  may not hold even if actuator faults do occur during the attitude maneuver.

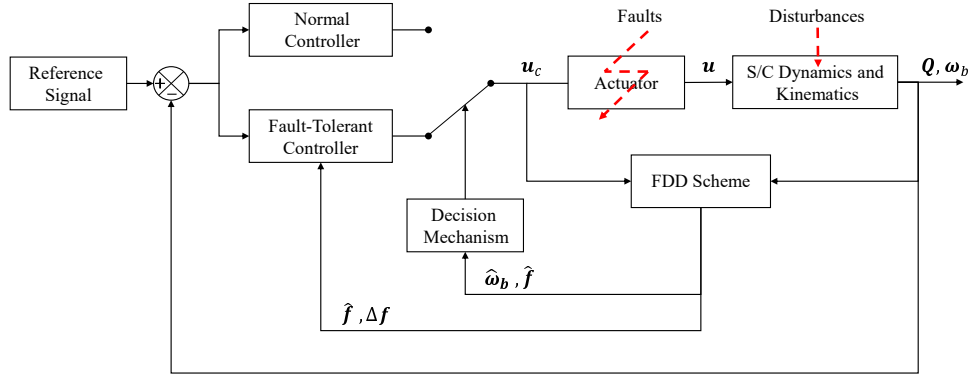


Fig. 1: Structure of the overall proposed active FTCS for attitude control system.

### B. Fault Estimation

After the fault is detected, we need to identify fault sizes and time characteristics subsequently. In this paper, we estimate the total fault effects in place of individual fault itself, so that the estimation algorithm is simple and requires less onboard computing power and memory space. To identify the total actuator faults  $\mathbf{f}$  in (4), an indirect fault identification scheme is proposed. First, introducing an auxiliary variable [28]:

$$\boldsymbol{\psi} = \mathbf{f} - \mathbf{G}\mathbf{J}\boldsymbol{\omega}_b, \quad (13)$$

where  $\mathbf{G} \in \mathbb{R}^{3 \times 3} > 0$  is a gain matrix. Taking time derivative of  $\boldsymbol{\psi}$ , we have

$$\dot{\boldsymbol{\psi}} = \dot{\mathbf{f}} - \mathbf{G}(-\mathbf{S}(\boldsymbol{\omega}_b)\mathbf{J}\boldsymbol{\omega}_b + \mathbf{D}\mathbf{u}_c + \mathbf{G}\mathbf{J}\boldsymbol{\omega}_b + \boldsymbol{\psi} + \mathbf{d}). \quad (14)$$

Let  $\hat{\boldsymbol{\psi}}$  and  $\hat{\mathbf{f}}$  be the estimates of  $\boldsymbol{\psi}$  and  $\mathbf{f}$  respectively, the indirect fault estimator is given as follows:

$$\mathbf{J}\dot{\hat{\boldsymbol{\omega}}}_{b,i} = -\mathbf{S}(\hat{\boldsymbol{\omega}}_{b,i})\mathbf{J}\hat{\boldsymbol{\omega}}_{b,i} + \mathbf{D}\mathbf{u}_c + \hat{\mathbf{f}} + \mathbf{L}(\boldsymbol{\omega}_b - \hat{\boldsymbol{\omega}}_{b,i}) \quad (15)$$

$$\dot{\hat{\boldsymbol{\psi}}} = -\mathbf{G}\hat{\boldsymbol{\psi}} - \mathbf{G}(-\mathbf{S}(\hat{\boldsymbol{\omega}}_{b,i})\mathbf{J}\hat{\boldsymbol{\omega}}_{b,i} + \mathbf{D}\mathbf{u}_c + \mathbf{G}\mathbf{J}\hat{\boldsymbol{\omega}}_{b,i}) \quad (16)$$

$$\hat{\mathbf{f}} = \hat{\boldsymbol{\psi}} + \mathbf{G}\mathbf{J}\hat{\boldsymbol{\omega}}_{b,i}, \quad (17)$$

where  $\hat{\boldsymbol{\omega}}_{b,i}$  is the angular velocity estimation in fault identification, and  $\mathbf{L} \in \mathbb{R}^{3 \times 3}$  is a positive-definite gain matrix. The term containing  $\boldsymbol{\omega}_b - \hat{\boldsymbol{\omega}}_{b,i}$  in (15) is a feedback input to ensure that the estimates converge to their true values. Define  $\tilde{\boldsymbol{\omega}}_{b,i} = \boldsymbol{\omega}_b - \hat{\boldsymbol{\omega}}_{b,i}$ ,  $\tilde{\boldsymbol{\psi}} = \boldsymbol{\psi} - \hat{\boldsymbol{\psi}}$ , and  $\tilde{\mathbf{f}} = \mathbf{f} - \hat{\mathbf{f}}$ , respectively. The error system is derived as

$$\mathbf{J}\dot{\tilde{\boldsymbol{\omega}}}_{b,i} = -\mathbf{S}(\boldsymbol{\omega}_b)\mathbf{J}\boldsymbol{\omega}_b + \mathbf{S}(\hat{\boldsymbol{\omega}}_{b,i})\mathbf{J}\hat{\boldsymbol{\omega}}_{b,i} + \tilde{\mathbf{f}} + \mathbf{d} - \mathbf{L}\tilde{\boldsymbol{\omega}}_{b,i} \quad (18)$$

$$\dot{\tilde{\boldsymbol{\psi}}} = \dot{\mathbf{f}} - \mathbf{G}\tilde{\boldsymbol{\psi}} + \mathbf{G}(\mathbf{S}(\boldsymbol{\omega}_b)\mathbf{J}\boldsymbol{\omega}_b - \mathbf{S}(\hat{\boldsymbol{\omega}}_{b,i})\mathbf{J}\hat{\boldsymbol{\omega}}_{b,i}) - \mathbf{G}^2\mathbf{J}\tilde{\boldsymbol{\omega}}_{b,i} \quad (19)$$

$$\dot{\tilde{\mathbf{f}}} = \dot{\boldsymbol{\psi}} + \mathbf{G}\mathbf{J}\tilde{\boldsymbol{\omega}}_{b,i}. \quad (20)$$

Based on the above error systems, the result for fault identification is delineated in the following.

**Theorem 2:** Considering the attitude dynamics in (4) with Assumptions 1-4. If there exist a matrix  $\mathbf{L}$  and a constant  $\mu > 0$  such that

$$\begin{bmatrix} \mathbf{L} - \mathbf{G}\mathbf{J} - \left(\ell_g + \frac{\epsilon}{2} + \frac{\epsilon}{2}\mu\ell_g^2\right)\mathbf{I}_3 & \mu\mathbf{G} - \frac{\mu}{\epsilon}\mathbf{G}\mathbf{G}^T \\ \frac{1}{2}(\mu\mathbf{J}^T(\mathbf{G}^2)^T - \mathbf{I}_3) & \mu\mathbf{G} - \frac{\mu}{\epsilon}\mathbf{G}\mathbf{G}^T \end{bmatrix} > 0$$

for given matrix  $\mathbf{G} > 0$  and constant  $\epsilon > 0$ , then the indirect fault identification approach proposed in (15)-(17) ensures that the total fault estimation error  $\tilde{\mathbf{f}}$  exponentially converges to a invariant set containing the origin.

*Proof.* Premultiplying (18) by  $\tilde{\boldsymbol{\omega}}_{b,i}^T$  leads to

$$\begin{aligned} \tilde{\boldsymbol{\omega}}_{b,i}^T \mathbf{J}\dot{\tilde{\boldsymbol{\omega}}}_{b,i} &\leq -\tilde{\boldsymbol{\omega}}_{b,i}^T \left( \mathbf{L} - \mathbf{G}\mathbf{J} - \left(\ell_g + \frac{\epsilon}{2}\right)\mathbf{I}_3 \right) \tilde{\boldsymbol{\omega}}_{b,i} \\ &\quad + \tilde{\boldsymbol{\omega}}_{b,i}^T \tilde{\boldsymbol{\psi}} + \frac{1}{2\epsilon}\bar{d}^2, \end{aligned} \quad (21)$$

where the inequality  $\tilde{\boldsymbol{\omega}}_{b,i}^T \mathbf{d} \leq \frac{\epsilon}{2}\tilde{\boldsymbol{\omega}}_{b,i}^T \tilde{\boldsymbol{\omega}}_{b,i} + \frac{1}{2\epsilon}\bar{d}^2$  is utilized.

In addition, according to (19) and Assumption 4, we have

$$\begin{aligned} \tilde{\boldsymbol{\psi}}^T \dot{\tilde{\boldsymbol{\psi}}} &\leq -\tilde{\boldsymbol{\psi}}^T \left( \mathbf{G} - \frac{1}{\epsilon}\mathbf{G}\mathbf{G}^T \right) \tilde{\boldsymbol{\psi}} - \tilde{\boldsymbol{\psi}}^T \mathbf{G}^2 \mathbf{J}\tilde{\boldsymbol{\omega}}_{b,i} \\ &\quad + \frac{\epsilon}{2}\ell_g^2 \tilde{\boldsymbol{\omega}}_{b,i}^T \tilde{\boldsymbol{\omega}}_{b,i} + \frac{\epsilon}{2}\phi^2 + \frac{\epsilon}{2}\bar{d}^2, \end{aligned} \quad (22)$$

where the following inequalities

$$\tilde{\boldsymbol{\psi}}^T \tilde{\mathbf{f}} \leq \frac{1}{2\epsilon}\tilde{\boldsymbol{\psi}}^T \tilde{\boldsymbol{\psi}} + \frac{\epsilon}{2}\phi^2 \quad (23)$$

$$-\tilde{\boldsymbol{\psi}}^T \mathbf{G}\mathbf{d} \leq \frac{1}{2\epsilon}\tilde{\boldsymbol{\psi}}^T \mathbf{G}\mathbf{G}^T \tilde{\boldsymbol{\psi}} + \frac{\epsilon}{2}\bar{d}^2 \quad (24)$$

$$\begin{aligned} \tilde{\boldsymbol{\psi}}^T \mathbf{G}(\mathbf{S}(\boldsymbol{\omega}_b)\mathbf{J}\boldsymbol{\omega}_b - \mathbf{S}(\hat{\boldsymbol{\omega}}_{b,i})\mathbf{J}\hat{\boldsymbol{\omega}}_{b,i}) &\leq \\ \frac{1}{2\epsilon}\tilde{\boldsymbol{\psi}}^T \mathbf{G}\mathbf{G}^T \tilde{\boldsymbol{\psi}} &+ \frac{\epsilon}{2}\ell_g^2 \tilde{\boldsymbol{\omega}}_{b,i}^T \tilde{\boldsymbol{\omega}}_{b,i} \end{aligned} \quad (25)$$

are applied. Now, we construct a Lyapunov candidate as

$$V = \frac{1}{2}\tilde{\boldsymbol{\omega}}_{b,i}^T \mathbf{J}\tilde{\boldsymbol{\omega}}_{b,i} + \frac{\mu}{2}\tilde{\boldsymbol{\psi}}^T \tilde{\boldsymbol{\psi}}, \quad (26)$$

where  $\mu > 0$  is a design constant. The time derivative of  $V$  along with (21) and (22) is given as

$$\begin{aligned} \dot{V} &\leq -\tilde{\boldsymbol{\omega}}_{b,i}^T \left( \mathbf{L} - \mathbf{G}\mathbf{J} - \left(\ell_g + \frac{\epsilon}{2} + \frac{\epsilon}{2}\mu\ell_g^2\right)\mathbf{I}_3 \right) \tilde{\boldsymbol{\omega}}_{b,i} \\ &\quad - \mu\tilde{\boldsymbol{\psi}}^T \left( \mathbf{G} - \frac{1}{\epsilon}\mathbf{G}\mathbf{G}^T \right) \tilde{\boldsymbol{\psi}} - \tilde{\boldsymbol{\omega}}_{b,i}^T (\mu\mathbf{J}^T(\mathbf{G}^2)^T - \mathbf{I}_3) \tilde{\boldsymbol{\psi}} \\ &\quad + \frac{\epsilon}{2}\mu\phi^2 + \frac{\epsilon}{2}\mu\bar{d}^2 + \frac{1}{2\epsilon}\bar{d}^2. \end{aligned} \quad (27)$$

The foregoing inequality further results in

$$\dot{V} \leq -[\tilde{\boldsymbol{\omega}}_{b,i}^T \quad \tilde{\boldsymbol{\psi}}^T] \mathbf{P} [\tilde{\boldsymbol{\omega}}_{b,i}^T \quad \tilde{\boldsymbol{\psi}}^T]^T + \sigma, \quad (28)$$

where

$$\mathbf{P} = \begin{bmatrix} \mathbf{L} - \mathbf{G}\mathbf{J} - \left(\ell_g + \frac{\epsilon}{2} + \frac{\epsilon}{2}\mu\ell_g^2\right)\mathbf{I}_3 & \mu\mathbf{G} - \frac{\mu}{\epsilon}\mathbf{G}\mathbf{G}^T \\ \frac{1}{2}(\mu\mathbf{J}^T(\mathbf{G}^2)^T - \mathbf{I}_3) & \mu\mathbf{G} - \frac{\mu}{\epsilon}\mathbf{G}\mathbf{G}^T \end{bmatrix}$$

and  $\sigma = \frac{\epsilon}{2}\mu\phi^2 + \frac{\epsilon}{2}\mu\bar{d}^2 + \frac{1}{2\epsilon}\bar{d}^2$ . If the matrix  $\mathbf{P}$  is positive definite, i.e.,  $\mathbf{P} > 0$ , then we have

$$\dot{V} \leq -\kappa V + \sigma, \quad (29)$$

where  $\kappa = \frac{2\lambda_{\min}[\mathbf{Q}]}{\max\{J, \mu\}}$ . According to the Lyapunov stability theory [29], it can be concluded from (29) that  $\tilde{\omega}$  and  $\tilde{\psi}$  are uniformly bounded. Define an invariant set  $\mathcal{S}_{(\tilde{\omega}_{b,i}, \tilde{\psi})}$  as

$$\mathcal{S}_{(\tilde{\omega}_{b,i}, \tilde{\psi})} = \left\{ (\tilde{\omega}_{b,i}, \tilde{\psi}) \left| \frac{J}{2} \|\tilde{\omega}_{b,i}\|^2 + \frac{\mu}{2} \|\tilde{\psi}\|^2 \leq \sqrt{\frac{\sigma}{\kappa}} \right. \right\}, \quad (30)$$

and its corresponding supplementary set is notated as  $\bar{\mathcal{S}}_{(\tilde{\omega}_{b,i}, \tilde{\psi})}$ . Considering (29) again, it is obtained that  $\dot{V} \leq 0$  if  $(\tilde{\omega}_{b,i}, \tilde{\psi}) \in \bar{\mathcal{S}}_{(\tilde{\omega}_{b,i}, \tilde{\psi})}$ . Therefore, it is clear that the estimation errors  $(\tilde{\omega}_{b,i}, \tilde{\psi})$  converge to the invariant set  $\mathcal{S}_{(\tilde{\omega}_{b,i}, \tilde{\psi})}$  exponentially at a rate greater than  $e^{-\kappa t}$ . Moreover, in view of (20) which indicates the fault estimation error  $\tilde{\mathbf{f}}$  is a combination of  $\tilde{\omega}_{b,i}$  and  $\tilde{\psi}$ , the fault estimation error  $\tilde{\mathbf{f}}$  also converges to an invariant set exponentially. This completes the proof.  $\triangle \triangle \triangle$

**Remark 4:** As seen from (18)-(20), larger estimator gains  $\mathbf{L}$  and  $\mathbf{G}$  lead to faster convergence of estimation errors  $\tilde{\omega}_{b,i}$  and  $\tilde{\psi}$ . However,  $\mathbf{G}$  cannot be arbitrarily large due to the constraint in Theorem 2.

**Remark 5:** In practical aerospace engineering, the time allocated to fault identification is limited due to the mission requirement. However, the fault estimate may not be able to obtain the true value within this assigned time interval. A long process of fault identification may lead to system instability or severe performance degradation as no action is adopted to compensate fault effects during the fault identification [12]. To cope with this issue, we introduce a decision mechanism, where an identification threshold  $\xi_{it}$  is introduced to determine the fault estimation accuracy. If  $\|\tilde{\omega}_{b,i}(t)\| + \|\hat{\mathbf{f}}(t) - \hat{\mathbf{f}}(t - T)\| < \xi_{it}$  with sampling interval  $T$ , we conclude that the fault identification is completed and switch to the fault-tolerant controller from the normal controller. Otherwise, it is considered that the fault has not been estimated successfully. Noting that the smaller the threshold is set, the longer identification time is needed, but with a better fault estimation accuracy. The fault estimation accuracy further affects the control accuracy in fault-tolerant control design.

#### IV. FAULT-TOLERANT CONTROL

Once we have estimated faults successfully, a fault-tolerant controller using the estimated fault information should be proposed to compensate fault effects and recover the performance. Although the developed fault identification approach in the previous Section provides an accurate fault estimation, there may still exist estimation errors in the system due to the estimation threshold, measurement noises, and system perturbations/uncertainties.

To improve the robustness of the fault-tolerant controller, sliding mode control technique (see for example [30]–[32]) is one of the potential and powerful design approaches. Besides, if the commanded control torque is larger than the maximal torque the actuator is able to produce, some unpredictable

control actions or damages to the actuator may come up [33], especially when there exist actuator faults in the attitude control system. Therefore, actuator saturation constraints and fault estimation errors are taken into account in the fault-tolerant controller design.

**Assumption 5:** It is assumed that the available control torque generated by the actuator is limited by

$$|u_{ci}| \leq u_{\max}, \quad (i = 1, 2, \dots, n) \quad (31)$$

where  $u_{\max}$  is a common saturation value for all actuators.

Let  $\Delta \mathbf{f}$  be the estimation errors, which is defined as  $\Delta \mathbf{f} = \mathbf{f} - \hat{\mathbf{f}}$ . It is reasonable to assume that the estimation errors are bounded [20] after successful fault identification, i.e.,  $\|\Delta \mathbf{f}\| < \delta$  with a constant  $\delta > 0$ . Considering the fault estimation errors and recalling actuator saturation constraint ( $|u_{ci}| \leq u_{\max}$ ) in Assumption 5, the attitude dynamics in (4) is rewritten as

$$\mathbf{J}\dot{\omega}_b = -\omega_b^\times \mathbf{J}\omega_b + \mathbf{D}u_c^{\text{sat}} + \hat{\mathbf{f}} + \Delta \mathbf{f} + \mathbf{d}, \quad (32)$$

where  $u_c^{\text{sat}}$  denotes the constrained control input commanded by the controller. Define the pseudoinverse of matrix  $\mathbf{D}$  as  $\mathbf{D}^+ = \mathbf{D}^T(\mathbf{D}\mathbf{D}^T)^{-1}$ , which satisfies  $\mathbf{D}\mathbf{D}^+ = \mathbf{I}_3$ . Since  $\mathbf{D}$  is the assemble matrix decided by the spacecraft structure, the matrix  $\mathbf{D}$  is constant, and there exists a finite constant  $\varepsilon_0$  such that  $\|\mathbf{D}^+\| \leq \varepsilon_0$ . As illustrated in equation (32), the estimation error  $\Delta \mathbf{f}$  affects the control performance in a way similar to external disturbances. We have to accommodate it in fault-tolerant controller to improve robustness and control performance.

To derive the fault-tolerant controller, the following Lemma 1 is also used.

**Lemma 1:** For  $x \in [-1, 1]$ , if a positive constant  $\beta$  is selected to satisfy  $\beta \geq 1.5574$ , then we have

$$-\alpha x \arctan(\beta x) \leq -\alpha x^2, \quad (33)$$

where  $\alpha$  is a positive constant.

*Proof.* See the Appendix A.  $\triangle \triangle \triangle$

For the fault-tolerant controller design, the method of integrator backstepping is utilized. Considering the kinematics subsystem in (2), the angular velocity  $\omega_b$  is regarded as a virtual control input, which is designed as

$$\omega_c = -\alpha \arctan(\beta \mathbf{q}). \quad (34)$$

As a consequence, the virtual velocity error between  $\omega_b$  and  $\omega_c$  is defined as

$$\mathbf{s} = \omega_b - \omega_c = \omega_b + \alpha \arctan(\beta \mathbf{q}). \quad (35)$$

In contrast to works of [5], [6] with a linear virtual control input, the nonlinear one given in (34) overcomes several defects such as excessive torque demand at the beginning of maneuver and sluggish motion when the system state is near the equilibrium point [34].

Choosing a candidate Lyapunov function as

$$V_1 = k_0 \mathbf{q}^T \mathbf{q} + k_0 (1 - q_0)^2. \quad (36)$$

Applying Lemma 1, the derivative of  $V_1$  satisfies

$$\dot{V}_1 \leq -k_0 \alpha \|\mathbf{q}\|^2 + k_0 \alpha \mathbf{q}^T \mathbf{s}. \quad (37)$$

It is clear that  $\dot{V}_1 \leq 0$  if  $\mathbf{s} = 0$ .

Next, the attitude dynamics with respect to virtual velocity error  $\mathbf{s}$  is derived as

$$\begin{aligned} \mathbf{J}\dot{\mathbf{s}} &= \mathbf{J}\dot{\boldsymbol{\omega}}_b + \alpha\beta\mathbf{J}(\mathbf{I}_3 + \beta^2\boldsymbol{\Xi}_q)^{-1}\dot{\mathbf{q}} \\ &= -k_0\mathbf{q} + \mathbf{F}(\cdot) + \mathbf{D}\mathbf{u}_c^{\text{sat}} + \hat{\mathbf{f}}, \end{aligned} \quad (38)$$

where the nonlinear term  $\mathbf{F}(\cdot)$  is defined as

$$\begin{aligned} \mathbf{F}(\cdot) &= k_0\mathbf{q} - \boldsymbol{\omega}_b^\times \mathbf{J}\boldsymbol{\omega}_b + \Delta\mathbf{f} + \mathbf{d} \\ &+ \frac{1}{2}\alpha\beta\mathbf{J}(\mathbf{I}_3 + \beta^2\boldsymbol{\Xi}_q)^{-1}(\mathbf{S}(\mathbf{q}) + q_0\mathbf{I}_3)\boldsymbol{\omega}_b \end{aligned} \quad (39)$$

with  $\boldsymbol{\Xi}_q = \text{diag}(q_1^2, q_2^2, q_3^2)$ . According to Assumptions 1-2, we have

$$\|-\boldsymbol{\omega}_b^\times \mathbf{J}\boldsymbol{\omega}_b\| \leq \bar{J}\|\boldsymbol{\omega}_b\|^2, \quad (40)$$

$$\|k_0\mathbf{q} + \Delta\mathbf{f} + \mathbf{d}\| \leq k_0 + \delta + \bar{d}, \quad (41)$$

$$\left\| \frac{1}{2}\alpha\beta\mathbf{J}(\mathbf{I}_3 + \beta^2\boldsymbol{\Xi}_q)^{-1}(\mathbf{S}(\mathbf{q}) + q_0\mathbf{I}_3)\boldsymbol{\omega}_b \right\| \leq \frac{1}{2}\alpha\beta\bar{J}\|\boldsymbol{\omega}_b\|. \quad (42)$$

In view of foregoing three inequalities, it is clear that

$$\|\mathbf{F}(\cdot)\| \leq \bar{J}\|\boldsymbol{\omega}_b\|^2 + \frac{1}{2}\alpha\beta\bar{J}\|\boldsymbol{\omega}_b\| + k_0 + \delta + \bar{d} \leq h\Omega, \quad (43)$$

where  $h = \max\{\bar{J}, \frac{1}{2}\alpha\beta\bar{J}, k_0 + \delta + \bar{d}\}$ , and  $\Omega = \|\boldsymbol{\omega}_b\|^2 + \|\boldsymbol{\omega}_b\|^2 + 1$ . Since  $\bar{J}$  and  $\delta$  may be difficult to obtain, the variable  $h$  is assumed to be unknown. As a result,  $h$  cannot be used directly in fault-tolerant controller design.

Before we give the details of the fault-tolerant controller, the following assumption is introduced first.

**Assumption 6:** The following inequality holds

$$\frac{u_{\max}}{\varepsilon_0} \geq h\Omega + \|\hat{\mathbf{f}}\| + \varrho_0, \quad (44)$$

where  $\varrho_0$  is a small constant.

**Remark 6:** Assumption 6 implies that the functional actuators (even in the event of severe faults) are able to produce sufficient torque for the spacecraft to perform a required maneuver. Similar Assumptions can also be found in [13], [22], [30] when the actuation saturation is considered during the controller design.

Now, it is ready to give the fault-tolerant controller as

$$\mathbf{u}_c^{\text{sat}} = -\frac{u_{\max}}{\varepsilon_0}\mathbf{D}^+\text{sat}[\Gamma(\cdot)\mathbf{s}] \quad (45)$$

with

$$\Gamma(\cdot) = k + \frac{\mathbf{s}^T \hat{\mathbf{f}}}{\|\mathbf{s}\|^2 + \varepsilon_1^2} + \frac{\hat{h}\Omega}{\|\mathbf{s}\| + \varepsilon_2}, \quad (46)$$

where  $k$  and  $\varepsilon_1$  are two positive constants,  $\varepsilon_2 = \frac{\nu}{\Omega}$  with a small positive constant  $\nu$ , the function  $\text{sat}[\Gamma(\cdot)\mathbf{s}]$  is defined as

$$\text{sat}[\Gamma(\cdot)\mathbf{s}] = \begin{cases} \frac{\mathbf{s}}{\|\mathbf{s}\|}, & \text{if } \|\mathbf{s}\| \geq \frac{u_{\max}}{\varepsilon_0\Gamma(\cdot)} \\ \frac{\varepsilon_0\Gamma(\cdot)\mathbf{s}}{u_{\max}}, & \text{if } \|\mathbf{s}\| \leq \frac{u_{\max}}{\varepsilon_0\Gamma(\cdot)} \end{cases} \quad (47)$$

The adaptive law of  $\hat{h}$  is given by

$$\dot{\hat{h}} = -c_1\hat{h} + \frac{c_2\Omega\|\mathbf{s}\|^2}{\|\mathbf{s}\| + \varepsilon_2}, \quad (48)$$

where  $c_1$  and  $c_2$  are two positive constants. Although the function  $\text{sat}[\Gamma(\cdot)\mathbf{s}]$  defined in (47) is piecewise, it is continuous everywhere including at the point  $\|\mathbf{s}\| = \frac{u_{\max}}{\varepsilon_0\Gamma(\cdot)}$ . Therefore, the proposed fault-tolerant controller in (45) is also continuous.

**Theorem 3:** Consider the attitude kinematics and dynamics described by (1) and (2) subject to actuator faults modelled in (3) and input saturation. If the fault-tolerant controller developed in (45) to (48) is applied after successful fault identification, then the closed-loop system is uniformly ultimately bounded stable, and the attitude and virtual velocity errors converge to a small invariant set containing the origin.

*Proof.* To show the stability of the closed-loop under the saturated FTC scheme in (45) with adaptive law in (48), two cases in light of (47) need to be addressed.

*Case I:*  $\|\mathbf{s}\| \geq \frac{u_{\max}}{\varepsilon_0\Gamma(\cdot)}$ , the controller in (45) becomes

$$\mathbf{u}_c^{\text{sat}} = -\frac{u_{\max}}{\varepsilon_0}\mathbf{D}^+\frac{\mathbf{s}}{\|\mathbf{s}\|}. \quad (49)$$

Since  $\|\mathbf{D}^+\| \leq \varepsilon_0$ , it is clear that  $\|\mathbf{u}_c^{\text{sat}}\| \leq u_{\max}$ . As a consequence, the actuator saturation constraint in (31) is satisfied. Considering the Lyapunov candidate as

$$V_2 = V_1 + \frac{1}{2}\mathbf{s}^T \mathbf{J} \mathbf{s}. \quad (50)$$

Then, it follows that

$$\begin{aligned} \dot{V}_2 &\leq k_0\boldsymbol{\omega}_b^T \mathbf{q}_e + \mathbf{s}^T \left( -k_0\mathbf{q} + \mathbf{F}(\cdot) \right. \\ &\quad \left. - \mathbf{D} \left( \frac{u_{\max}}{\varepsilon_0}\mathbf{D}^+\frac{\mathbf{s}}{\|\mathbf{s}\|} \right) + \hat{\mathbf{f}} \right) \\ &\leq -k_0\alpha\|\mathbf{q}\|^2 - \frac{u_{\max}}{\varepsilon_0}\|\mathbf{s}\| + h\Omega\|\mathbf{s}\| + \|\hat{\mathbf{f}}\|\|\mathbf{s}\|. \end{aligned} \quad (51)$$

According to the inequality in Assumption 6, we have

$$\dot{V}_2 \leq -k_0\alpha\|\mathbf{q}\|^2 - \varrho_0\|\mathbf{s}\| < 0. \quad (52)$$

*Case II:*  $\|\mathbf{s}\| \leq \frac{u_{\max}}{\varepsilon_0\Gamma(\cdot)}$ , the controller in (45) becomes

$$\mathbf{u}_c^{\text{sat}} = -\Gamma(\cdot)\mathbf{D}^+\mathbf{s}. \quad (53)$$

Another Lyapunov candidate is chosen as

$$V_2 = V_1 + \frac{1}{2}\mathbf{s}^T \mathbf{J} \mathbf{s} + \frac{1}{2c_2}\hat{h}^2. \quad (54)$$

The time derivative of (54) is

$$\begin{aligned} \dot{V}_2 &\leq -k_0\alpha\|\mathbf{q}\|^2 + \mathbf{s}^T \left( \mathbf{F}(\cdot) - \left( k\mathbf{s} + \frac{\mathbf{s}^T \hat{\mathbf{f}} \mathbf{s}}{\|\mathbf{s}\|^2 + \varepsilon_1^2} \right. \right. \\ &\quad \left. \left. + \frac{\hat{h}\Omega\mathbf{s}}{\|\mathbf{s}\| + \varepsilon_2} \right) + \hat{\mathbf{f}} \right) + \frac{1}{c_2}\hat{h}\dot{\hat{h}} \\ &\leq -k_0\alpha\|\mathbf{q}\|^2 - k\|\mathbf{s}\|^2 - \frac{c_1}{2c_2}\hat{h}^2 + \eta, \end{aligned} \quad (55)$$

where  $\eta = \frac{\varepsilon_1}{2}\|\hat{\mathbf{f}}\| + \nu h + \frac{c_1}{2c_2}h^2 < \infty$  as  $\|\mathbf{s}\|^2 + \varepsilon_1^2 \geq 2\varepsilon_1\|\mathbf{s}\|$  and  $\varepsilon_2 = \frac{\nu}{\Omega}$ . It follows from the foregoing inequality that

$$\dot{V}_2 \leq -\gamma V_2 + \zeta, \quad (56)$$

where  $\gamma = \min\{k_0\alpha, \frac{k}{J}, c_1\}$  and  $\zeta = \frac{\varepsilon_1}{2}\|\hat{\mathbf{f}}\| + \nu h + \frac{c_1}{2c_2}h^2 + k_0\alpha(1 - q_0^2) < \infty$ . Therefore, the closed-loop system is ultimately bounded stable and all the internal signals are

bounded. Furthermore, according (55), it is clear that  $\dot{V}_2 < 0$  if  $\|\mathbf{q}\| > \sqrt{\frac{\eta}{k_0\alpha}}$  or  $\|\mathbf{s}\| > \sqrt{\frac{\eta}{k}}$ . As a consequence, we conclude that the attitude  $\mathbf{q}$  and the virtual velocity error  $\mathbf{s}$  are ultimately stabilized to invariant sets

$$\mathcal{S}_q = \left\{ \mathbf{q} \mid \|\mathbf{q}\| \leq \sqrt{\frac{\eta}{k_0\alpha}} \right\} \quad \text{and} \quad \mathcal{S}_s = \left\{ \mathbf{s} \mid \|\mathbf{s}\| \leq \sqrt{\frac{\eta}{k}} \right\},$$

respectively. This completes the proof.  $\triangle \triangle \triangle$

**Remark 7:** According to the adaptive law in (48), the positive constant  $c_1$  mainly determines the increasing rate of the parameter  $\hat{h}(t)$  (the rising phase of  $\hat{h}(t)$  if the initial value  $\hat{h}(0)$  is small), while  $c_2$  adjusts the decreasing rate (the steady phase of  $\hat{h}(t)$ ). To have a smooth variation of the  $\hat{h}(t)$ , the design parameters  $c_1$  and  $c_2$  should be selected as small constants.

**Remark 8:** The closed-loop stability and control performance can be ensured by adjusting the design parameters  $k_0$ ,  $\alpha$ ,  $k$ ,  $\varepsilon_1$ , and  $\nu$ . It is observed from stability analysis that larger  $k_0$ ,  $\alpha$ , and  $k$  may result in faster convergence rate and smaller steady-state errors. Moreover, according to the ultimate error sets, the steady-state errors could be further reduced by decreasing design parameters  $\varepsilon_1$  and  $\nu$  in  $\eta$ . However,  $\varepsilon_1$  and  $\nu$  cannot be too small as they are also used for alleviating control chattering.

## V. SIMULATION RESULTS

To demonstrate the effectiveness and performance of the proposed FTCS design, numerical simulation is performed to a rigid spacecraft in this section. The inertia matrix of a rigid spacecraft is selected as  $\mathbf{J} = [10, 1.2, 0.5; 1.2, 19, 1.5; 0.5, 1.5, 25]$  [35]. External disturbance is assumed to be  $\mathbf{d}(t) = [-0.005 \sin(t), 0.005 \sin(t), -0.005 \sin(t)]^T$  N·m [36]. In the simulation, four reaction wheels in a pyramid configuration are used to provide control torques for attitude control, and the actuator distribution matrix is  $\mathbf{D} = [-1, -1, 1, 1; 1, -1, -1, 1; 1, 1, 1, 1]$ . Due to the physical limitation of reaction wheel, the maximal control torque is set to be 0.2 N·m. The spacecraft is assumed to have the initial angular velocity  $\boldsymbol{\omega}_b(0) = [0.005, 0.006, 0.004]^T$  rad/s and initial attitude  $\mathbf{Q}(0) = [-0.5, 0.3, -0.4, 0.7071]^T$ . The measurement bias of gyro is assumed to be  $1^\circ/h$  on each axis. In addition, in light of the limited manufacturing tolerances, we also consider the installation misalignments, which are  $0.005^\circ$  and  $0.1^\circ$  for attitude sensor and angular velocity sensor is, respectively. The fault scenario in the simulation is that the first and the second reaction wheel experience loss of effectiveness fault at  $t = 5$  s with  $e_1 = 0.6$  and  $e_2 = 0.2$ , while the additive bias fault happens to the second and the third reaction wheels at  $t = 100$  s with  $u_{a2} = -0.03$  N·m,  $u_{a3} = -0.04$  N·m.

To detect the actuator fault, the gain matrix of fault detection observer in (5) is selected as  $\boldsymbol{\Lambda} = 5\mathbf{I}_3$ . In addition, the fault detection threshold is chosen as  $\xi = 0.002$ . The design parameters of the fault identification scheme in (15) to (17) are selected as  $\mathbf{G} = 0.5\mathbf{I}_3$ ,  $\epsilon = 5$ , and  $\ell_g = 3$ . Sequentially,

solving the inequality in Theorem 2 via LMI toolbox in Matlab yields

$$\mathbf{L} = \begin{bmatrix} 16.7621 & 0.2 & 0 \\ 1 & 21.2621 & 0.5 \\ 0.5 & 1 & 24.2621 \end{bmatrix} \quad \text{and} \quad \mu = 0.2333.$$

To accommodate actuator faults, the control gains of adaptive fault-tolerant controller in (45) to (48) are chosen as  $\alpha = 0.2$ ,  $\beta = 1.8$ ,  $k = 100$ ,  $\varepsilon_1 = 0.1$ ,  $\nu = 0.01$ ,  $c_1 = 0.01$ , and  $c_2 = 0.1$ . The initial value for the adaptive parameter is chosen as  $\hat{h}(0) = 0.1$ . In the simulation, we set the fault detection threshold as  $\xi_{dt} = 0.002$ , which is obtained through trial and error to ensure the threshold is proper for fault detection.

Recalling the overall FTCS structure in Fig. 1, the normal controller for healthy-actuator case in simulation is design as

$$\mathbf{u}_c = -\mathbf{D}^+(k_p \mathbf{J} \mathbf{q} + k_d \mathbf{J} \boldsymbol{\omega}_b), \quad (57)$$

where control gains are selected as  $k_p = 0.1422$  and  $k_d = 0.5333$  such that the closed-loop attitude control system in healthy condition is critical damping. It is noted that the normal controller given in (57) is a proportional-derivative (PD) controller with pseudoinverse-based control allocation. To satisfy the actuator saturation constraint, we also limit the magnitude of the normal controller to less than 0.2 N·m.

As illustrated in Fig. 2a, the fault detection residual is less than the threshold  $\xi$  before fault occurs but increases conspicuously beyond the threshold once actuator faults occur at 5 s and 100 s. It is observed that the partial loss of effectiveness fault and additive bias fault are detected at 6.8 s and 100.6 s, respectively. In this simulation, we set the identification threshold as  $\xi_{it} = 0.002$ . According to Remark 5, we switch to the fault-tolerant controller from the normal controller if the condition  $\|\tilde{\boldsymbol{\omega}}_{b,i}(t)\| + \|\hat{\mathbf{f}}(t) - \hat{\mathbf{f}}(t-T)\| < \xi_{it}$  is satisfied. According to Figs. 2b and 2c, both the fault estimation error and angular velocity estimation error converge to a vicinity of zero ultimately. Noting that there is a small increase in the responses of fault and angular velocity estimation error after 100 s, which is due to the occurrence of the additive faults. To compensate the additive faults, as shown in Fig. 2f, the proposed fault-tolerant controller keeps commanding a non-zero control torque after 100 s. The responses of spacecraft attitude and angular velocity are shown in Figs. 2d and 2e, from which it is observed that fairly good control performance is achieved with the pointing accuracy 0.2 deg and stabilization accuracy  $6.6 \times 10^{-5}$  rad/s. Referring to Fig. 2f, the control torque commanded by the proposed controller is also constrained to less than 0.2 N·m. It is obvious that the fault-tolerant controller compensates the actuator fault effects especially after the occurrence of additive bias faults.

For comparison purposes, the PD controller designed in (57) and the traditional backstepping controller with a linear virtual input [6] are also performed. The traditional backstepping controller is designed to have the same structure as the proposed fault-tolerant controller except that the nonlinear virtual control input  $\boldsymbol{\omega}_c = -\alpha \arctan(\beta \mathbf{q})$  is replaced by the linear virtual control input  $\boldsymbol{\omega}_c = -\alpha \mathbf{q}$ . As shown in Fig. 3, the steady-state errors for attitude and angular velocity under PD controller are 2.8 deg and  $5.1 \times 10^{-4}$  rad/s, which is

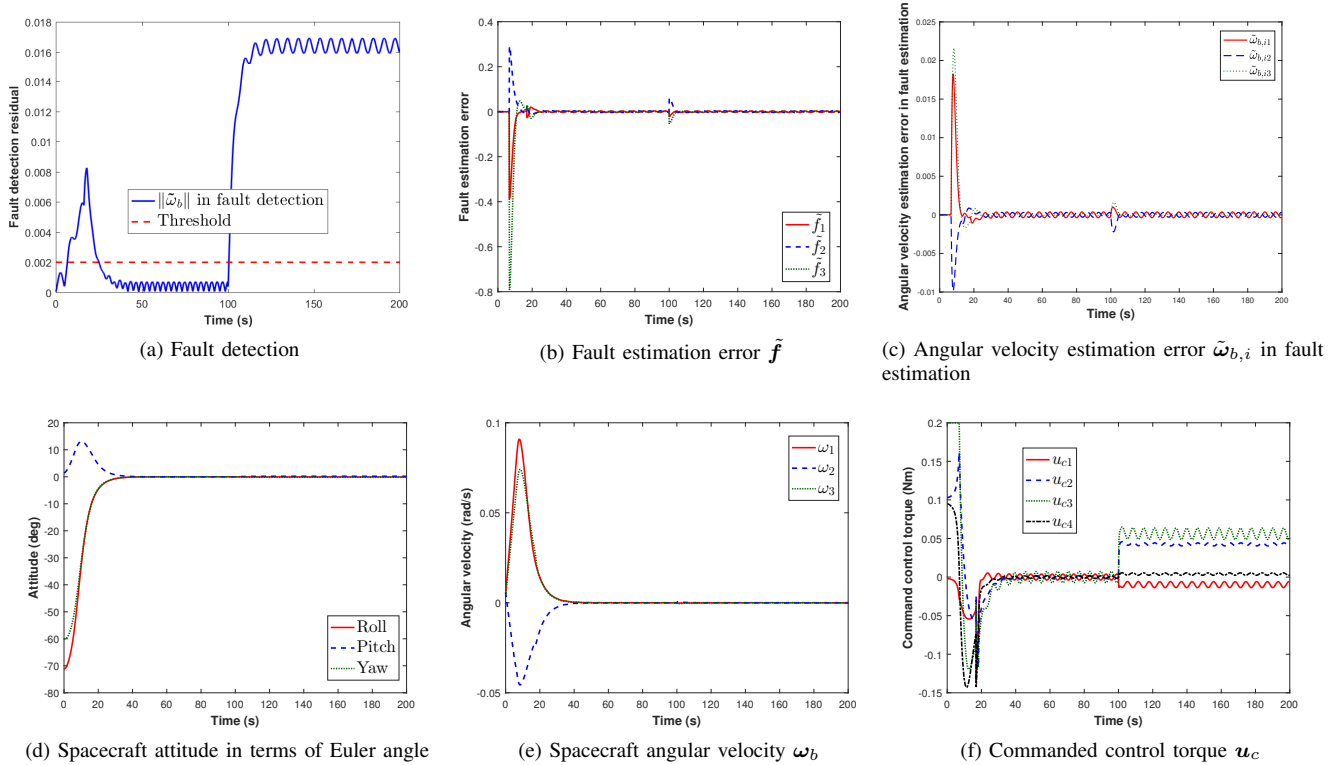


Fig. 2: Time responses of the proposed active FTCS in the presence of fault.

significantly worse than the proposed fault-tolerant controller with smaller steady-state errors. The responses of attitude and angular velocity under the traditional backstepping controller with a linear virtual input are shown in Fig. 4, in which an obvious sluggish motion is observed when the state errors are small. From the view point of the settling time, the proposed approach can converge the attitude and angular velocity to the error bounds  $|q_i(t)| \leq 0.2$  deg and  $|\omega_i| \leq 2 \times 10^{-4}$  rad/s in 36.9 s and 43.6 s, respectively, while the traditional backstepping controller requires 55.0 s and 61.8 s to reach the same attitude and angular velocity error bounds. Therefore, the settling time of the attitude and angular velocity with the proposed fault-tolerant controller is reduced by 49.1% and 41.7%, respectively. Therefore, it is verified that the proposed FTCS significantly improves the system performance.

## VI. CONCLUSION

In this paper, an active FTCS design is developed for spacecraft attitude control systems suffering from actuator faults. A fault detection scheme is proposed to determine the time at which the system is subject to actuator faults and false alarms are avoided from external disturbances. To have a simple structure of fault identification, the total fault effects are estimated in place of each individual fault. The developed indirect fault identification approach is able to exponentially estimate the total fault effects to the desired degree of accuracy. Subsequently, based on the estimated information about actuator faults, fault-tolerant control law is synthesized to accommodate actuator faults and saturation constraints.

The effectiveness of the proposed FTCS approach has been illustrated by simulation results. The future works may focus on reducing/avoiding the adverse transient in switching the control strategy from normal controller to reconfigurable one after the fault is identified successfully. One of the potential approaches for solving the switching transient is the technique presented in [37]. Moreover, to improve the sensitivity of the fault detection, time-varying fault detection threshold [38] should also be addressed.

## APPENDIX A: PROOF OF LEMMA 1

To prove Lemma 1, we first consider the case when  $x \in [0, 1]$ . The inequality  $-\alpha x \arctan(\beta x) \leq -\alpha x^2$  is equivalent to  $\arctan(\beta x) \geq x$  for  $x \in [0, 1]$ . Defining a function  $f(x) = \arctan(\beta x) - x$ , our aim is to show  $f(x) \geq 0$ . Taking derivatives of  $f(x)$  with respect to  $x$ , we have  $\frac{df(x)}{dx} = \frac{-\beta^2 x^2 + \beta - 1}{1 + \beta^2 x^2}$ . Then, we have  $\lim_{x \rightarrow 0^+} \frac{df(x)}{dx} = \beta - 1 > 0$  and  $\lim_{x \rightarrow 1^-} \frac{df(x)}{dx} = \frac{-\beta^2 - 1 + \beta}{1 + \beta^2} \leq \frac{-\beta}{1 + \beta^2} < 0$  if  $\beta \geq 1.5574$ . Next, for  $x \in (0, 1)$ , the second derivative is further obtained as  $\frac{d^2 f(x)}{dx^2} = \frac{-2\beta^3 x}{(1 + \beta^2 x^2)^2} < 0$ , which implies  $f(x)$  is strictly concave. Since  $f(x)$  is strictly concave for  $x \in (0, 1)$ ,  $\lim_{x \rightarrow 0^+} \frac{df(x)}{dx} > 0$ , and  $\lim_{x \rightarrow 1^-} \frac{df(x)}{dx} < 0$ , the minimum of  $f(x)$  is obtained at  $f(0)$  or  $f(1)$ . In view of  $f(0) = 0$ , it is clear  $f(x) \geq 0$  if  $f(1) \geq 0$ . Recalling  $\beta \geq 1.5574$ , it is easy to verify  $f(1) = \arctan(\beta) - 1 \geq 0$ . Therefore, the result  $-\alpha x \arctan(\beta x) \leq -\alpha x^2$  is established for  $x \in [0, 1]$ . As both  $\alpha x \arctan(\beta x)$  and  $\alpha x^2$  are even functions, the result also holds when  $x \in [-1, 0]$ . This completes the proof.  $\triangle \triangle \triangle$

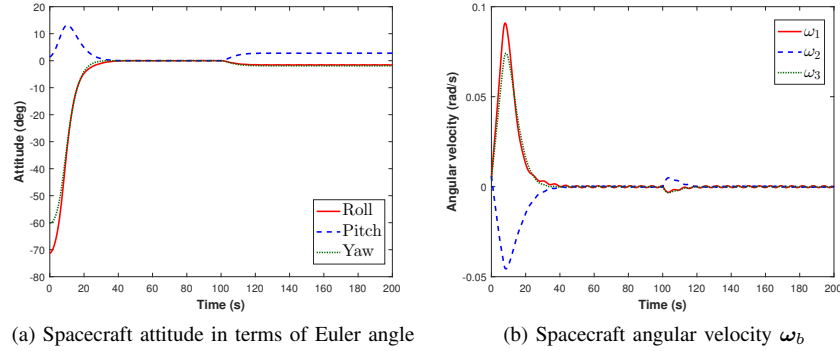


Fig. 3: Time responses of attitude control systems using only PD controller in the presence of fault.

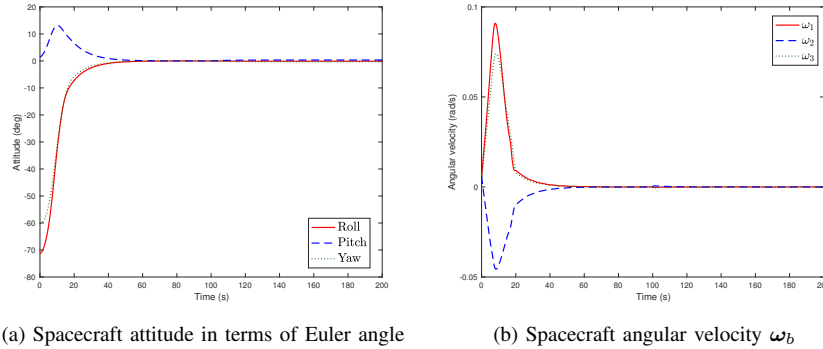


Fig. 4: Time responses of attitude control systems using the traditional backstepping controller with a linear virtual control input [6] in the presence of fault.

## REFERENCES

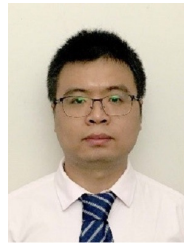
- [1] M. Blanke, R. Izadi-Zamanabadi, S. A. Bosh, and C. P. Lunau, "Fault-tolerant control systems - a holistic view," *Control Engineering Practice*, vol. 5, no. 5, pp. 693–702, May. 1997.
- [2] S. X. Ding, *Model-based Fault Diagnosis Techniques: Design Schemes, Algorithms, and Tools*. Berlin Heidelberg: Springer Science & Business Media, 2008.
- [3] Y. M. Zhang and J. Jiang, "Bibliographical review on reconfigurable fault-tolerant control systems," *Annual Reviews in Control*, vol. 32, no. 2, pp. 229–252, Dec. 2008.
- [4] S. Yin, B. Xiao, S. X. Ding, and D. H. Zhou, "A review on recent development of spacecraft attitude fault tolerant control system," *IEEE Transactions on Industrial Electronics*, vol. 63, no. 5, pp. 3311–3320, 2016.
- [5] W. Luo, Y.-C. Chu, and K.-V. Ling, "Inverse optimal adaptive control for attitude tracking of spacecraft," *IEEE Transactions on Automatic Control*, vol. 50, no. 11, pp. 1639–1654, Nov. 2005.
- [6] R. Kristiansen, P. J. Nicklasson, and J. T. Gravdahl, "Satellite attitude control by quaternion-based backstepping," *IEEE Transactions on Control Systems Technology*, vol. 17, no. 1, pp. 227–232, 2009.
- [7] L. Sun and Z. Zheng, "Disturbance-observer-based robust backstepping attitude stabilization of spacecraft under input saturation and measurement uncertainty," *IEEE Transactions on Industrial Electronics*, vol. 64, no. 10, pp. 7994–8002, Oct. 2017.
- [8] J. D. Boskovic, S. Li, and R. K. Mehra, "Robust tracking control design for spacecraft under control input saturation," *Journal of Guidance, Control, and Dynamics*, vol. 27, no. 4, pp. 627–633, Jan.-Feb. 2004.
- [9] Z. Zhu, Y. Q. Xia, and M. Y. Fu, "Adaptive sliding mode control for attitude stabilization with actuator saturation," *IEEE Transactions on Industrial Electronics*, vol. 58, no. 10, pp. 4898–4907, Oct. 2011.
- [10] J. T. Y. Wen and K. Kreutz-Delgado, "The attitude control problem," *IEEE Transactions on Automatic Control*, vol. 36, no. 10, pp. 1148–1162, 1991.
- [11] B. Xiao, S. Yin, and L. Wu, "A structure simple controller for satellite attitude tracking maneuver," *IEEE Transactions on Industrial Electronics*, vol. 64, no. 2, pp. 1436–1446, Feb. 2017.
- [12] J. Jiang and X. Yu, "Fault-tolerant control systems: A comparative study between active and passive approaches," *Annual Reviews in Control*, vol. 36, no. 1, pp. 60–72, Apr. 2012.
- [13] A.-M. Zou and K. D. Kumar, "Robust attitude coordination control for spacecraft formation flying under actuator failures," *Journal of Guidance, Control, and Dynamics*, vol. 35, no. 4, pp. 1247–1255, Jul.-Aug. 2012.
- [14] Q. Shen, D. W. Wang, S. Q. Zhu, and E. K. Poh, "Integral-type sliding mode fault-tolerant control for attitude stabilization of spacecraft," *IEEE Transactions on Control Systems Technology*, vol. 23, no. 3, pp. 1131–1138, 2015.
- [15] Q. Shen, D. W. Wang, S. Q. Zhu, and E. K. Poh, "Finite-time fault-tolerant attitude stabilization with actuator saturation," *IEEE Transactions on Aerospace and Electronic Systems*, vol. 51, no. 3, pp. 2390–2405, 2015.
- [16] G. Sun, S. Xu, and Z. Li, "Finite-time fuzzy sampled-data control for nonlinear flexible spacecraft with stochastic actuator failures," *IEEE Transactions on Industrial Electronics*, vol. 64, no. 5, pp. 3851–3861, 2017.
- [17] B. Xiao, X. Yang, and Y. Zhang, "Fault-tolerant attitude stabilization for satellites without rate sensor," *IEEE Transactions on Industrial Electronics*, vol. 62, no. 11, pp. 7191–7202, 2015.
- [18] P. Baldi, M. Blanke, P. Castaldi, M. N., and S. Simani, "Adaptive ftc based on control allocation and fault accommodation for satellite reaction wheel," in *Proceedings of the 3rd Conference on Control and Fault-Tolerant Systems*, pp. 672–677. IEEE, Piscataway, NJ, 2016.
- [19] B. Xiao and S. Yin, "Velocity-free fault-tolerant and uncertainty attenuation control for a class of nonlinear systems," *IEEE Transactions on Industrial Electronics*, vol. 63, no. 7, pp. 4400–4411, 2016.
- [20] S. Q. Zhu, D. W. Wang, Q. Shen, and E. K. Poh, "Satellite attitude stabilization control with actuator faults," *Journal of Guidance, Control, and Dynamics*, vol. 40, no. 5, pp. 130–1313, 2017.
- [21] S. P. Bhat and D. S. Bernstein, "A topological obstruction to con-

tinuous global stabilization of rotational motion and the unwinding phenomenon,” *Systems & Control Letters*, vol. 39, no. 1, pp. 63–70, 2000.

- [22] W. C. Cai, X. H. Liao, and Y. D. Song, “Indirect robust adaptive fault-tolerant control for attitude tracking of spacecraft,” *Journal of Guidance, Control, and Dynamics*, vol. 31, no. 5, pp. 1456–1463, Sep.–Oct. 2008.
- [23] B. Xiao, Q. L. Hu, and Y. M. Zhang, “Fault-tolerant attitude control for flexible spacecraft without angular velocity magnitude measurement,” *Journal of Guidance, Control, and Dynamics*, vol. 34, no. 5, pp. 1556–1561, 2011.
- [24] B. Wie and P. M. Barba, “Quaternion feedback for spacecraft large angle maneuvers,” *Journal of Guidance, Control, and Dynamics*, vol. 8, no. 3, pp. 360–365, 1985.
- [25] B. Wie, *Space Vehicle Dynamics and Control*. VA Reston: AIAA Education Series, 2008.
- [26] Q. Shen, C. F. Yue, C. H. Goh, B. L. Wu, and D. W. Wang, “Rigid-body attitude stabilization with attitude and angular rate constraint,” *Automatica*, vol. 90, pp. 157–163, 2018.
- [27] W. Chen and M. Saif, “Observer-based fault diagnosis of satellite systems subject to time-varying thruster faults,” *Journal of Dynamic Systems, Measurement, and Control*, vol. 129, no. 3, pp. 352–356, May, 2007.
- [28] J. W. Zhu, G. H. Yang, H. Wang, and F. L. Wang, “Fault estimation for a class of nonlinear systems based on intermediate estimator,” *IEEE Transactions on Automatic Control*, vol. 61, no. 9, pp. 2518–2524, 2016.
- [29] H. K. Khalil, *Nonlinear Systems*, 2nd ed. Upper Saddle, River, NJ: Prentice-Hall, 2002.
- [30] J. D. Boskovic, S. Li, and R. K. Mehra, “Robust adaptive variable structure control of spacecraft under control input saturation,” *Journal of Guidance, Control, and Dynamics*, vol. 24, no. 1, pp. 14–22, Jul.–Aug. 2001.
- [31] Y. Wang, Y. Gao, H. R. Karimi, H. Shen, and Z. Fang, “Sliding mode control of fuzzy singularly perturbed systems with application to electric circuit,” *IEEE Transactions on Systems, Man, and Cybernetics: Systems*, DOI 10.1109/TIE.2017.2772192, 2017, available online.
- [32] Y. Wang, Y. Xia, H. Shen, and Z. Pingfang, “Smc design for robust stabilization of nonlinear markovian jump singular systems,” *IEEE Transactions on Automatic Control*, vol. 63, no. 1, pp. 219–224, Jan. 2018.
- [33] W. E. Dixon, “Adaptive regulation of amplitude limited robot manipulators with uncertain kinematics and dynamics,” *IEEE Transactions on Automatic Control*, vol. 52, no. 3, pp. 488–493, 2007.
- [34] K. Kim and Y. Kim, “Robust backstepping control for slew maneuver using nonlinear tracking function,” *IEEE Transactions on Control Systems Technology*, vol. 11, no. 6, pp. 822–829, 2003.
- [35] A. Chunodkar and M. Akella, “Switching angular velocity observer for rigid-body attitude stabilization and tracking control,” *Journal of Guidance, Control, and Dynamics*, vol. 37, no. 3, pp. 869–878, 2014.
- [36] A. W. D. I. Thomas and H. S., “Variable-structure control of spacecraft attitude maneuvers,” *Journal of Guidance, Control, and Dynamics*, vol. 11, no. 3, pp. 262–270, 1988.
- [37] X. Yu, Y. M. Zhang, and Z. X. Liu, “Fault-tolerant control design with explicit consideration of reconfiguration transients,” *Journal of Guidance, Control, and Dynamics*, vol. 39, no. 3, pp. 556–563, Mar. 2016.
- [38] R. J. Patton and J. Chen, *Fault diagnosis in dynamic systems: Theory and Application*. Englewood Cliffs: Prentice-Hall, 1989.



**Qiang Shen** (S’12-M’16) received his B.E. degree in automation from the Northwestern Polytechnical University, Xi’an, China, in 2010 and the Ph.D degree from Nanyang Technological University, Singapore, in 2016. From 2015 to 2016, he held an Associate Scientist position at Temasek Laboratories, National University of Singapore, Singapore, and then a Research Scientist position at the same Laboratories from 2016 to 2017. He is currently a Postdoctoral Research Associate with the School for Engineering of Matter, Transport and Energy, Arizona State University, Tempe, AZ, USA. His research interests include active model discrimination, fault tolerant control, and control allocation.



elling and simulation using control moment gyros and adaptive control.

**Chengfei Yue** (S’16) received a B.Eng. degree in Flight Vehicle Design and Engineering from Honor School, Harbin Institute of Technology, Harbin, P.R.C in 2013. From Sep. 2017 to Dec. 2017, he was a visiting PhD student at Ryerson University, Canada. He is currently pursuing a Ph.D. degree with the Department of Electrical and Computer Engineering, National University of Singapore, Singapore. His current research interests include under-actuated attitude control of spacecraft, fault-tolerant control system, modelling and simulation using control moment gyros and adaptive control.



**Cher Hiang Goh** (SM’11) received his Diplom-Ingenieur (M.Sc.) and Doktor-Ingenieur (Ph.D) Degrees from Universitaet Paderborn (Germany) and Ruhr-Boechum Universitaet (Germany) in 1983 and 1993 respectively, while under government scholarship. He is currently a Distinguished Member of Technical Staff of DSO National Laboratories. He is also a Professor to National University of Singapore (NUS). He is the director of Singapore 1st Micro-satellite project (X-Sat) and led a team of about 50 engineers to successfully design, develop and launch the micro-satellite in 2011. He was a Distinguished Visiting Professor to Naval Postgraduate School of U.S.A. in 2012. From 2013 to 2016, he was seconded to National University of Singapore. There he led the space systems R&Ds as projects Principal Investigator and also the Director of the Satellite and Airborne Radar Systems Laboratory (SARSL). In DSO, he held various positions such as Programme Manager and Research Head (Guidance & Control Laboratory). He chaired the 1st Singapore Space Symposium in 2014 and is also General Co-Chair of IEEE Asia Pacific Synthetic Aperture Radar Conference 2015. He is a Senior Member of IEEE and also a Senior Member of AIAA. His technical and research interest are in the area of Guidance & Control; Space Systems Engineering and Developments.



**Danwei Wang** (S’88-M’89-SM’04) received his Ph.D and MSE degrees from the University of Michigan, Ann Arbor in 1989 and 1984, respectively. He received his B.E degree from the South China University of Technology, China in 1982. He is professor in the School of Electrical and Electronic Engineering, Nanyang Technological University, Singapore. He is director of the ST-NTU Corp Lab, NTU. He has served as head, Division of Control and Instrumentation from 2005 to 2011 and director of the Centre for Centre for System Intelligence and Efficiency until 2016. He also served as general chairman, technical chairman and various positions in international conferences. He has served as an associate editor of Conference Editorial Board, IEEE Control Systems Society. He is an associate editor of International Journal of Humanoid Robotics and invited guest editor of various international journals. He was a recipient of Alexander von Humboldt fellowship, Germany. He has published widely in the areas of iterative learning control, repetitive control, fault diagnosis and failure prognosis, satellite formation dynamics and control, as well as manipulator/mobile robot dynamics, path planning, and control.